IEEE Access
Multidisciplinary ⋮ Rapid Review ⋮ Open Access Journal

Received January 17, 2021, accepted January 31, 2021, date of publication February 3, 2021, date of current version February 12, 2021.

Digital Object Identifier 10.1109/ACCESS.2021.3056796

Modeling and Analysis of a Linear Generator for High Speed Maglev Train

SANSAN DING[1], WEITAO HAN[1], JINJI SUN[2], FUJIE JIANG[1], GUIMEI DENG[1], AND YUNQI SHI[1]

[1]CRRC Qingdao Sifang Company Ltd., Qingdao 266111, China
[2]School of Instrumentation Science and Opto-Electronics Engineering, Beihang University, Beijing 100191, China

Corresponding author: Jinji Sun (sunjinji2001@163.com)

This work was supported in part by the National Key Research and Development Program of China under Grant 2016YFB1200602, and in part by the National Natural Science Foundation of China under Grant 52075017 and Grant 62073010.

ABSTRACT This paper investigates a linear generator (LIG) for application in high speed maglev train. Its configuration and working principle are introduced in detail. The mathematic models of magnetic field and induced voltage are established by the equivalent magnetic circuit method and the law of electromagnetic induction respectively, through which the characteristics of LIG and impact factors are analyzed preliminarily. An analytical and numerical method is proposed to analyze the characteristics of LIG further, in which the finite element model is applied to calculate the magnetic field accurately and the analytical model is used for the induced voltage calculation in a discrete way. The relationships of induced voltage amplitude and speed, induced voltage frequency and speed are clarified, providing the basis for the design of power supply system on vehicle. Finally, the experiments for the magnetic field and induced voltage are carried out on the performance test bench of magnet and real vehicle respectively to validate the analysis results.

INDEX TERMS Linear generator, maglev train, analytical and numerical method, induced voltage.

I. INTRODUCTION

Magnetic suspension technology is employed in the realm of high speed rotation and linear motion gradually due to the advantageous of no friction, micro vibration, high precision and long service life. As a key component, the magnetic bearing is usually applied in the high rotating motion, such as magnetically suspended flywheel, magnetically suspended control moment gyroscope and magnetically suspended motor [1]–[3]. For the linear motion, the magnets which can accomplish levitation and guidance function play an important role in maglev elevator and maglev train. Especially for the maglev train, the technology has been researched for ages and realized commercial operation in many countries, such as China, German, Japan, South Korea and so on [4]–[6]. According to the speed level, maglev train can be divided into the middle-low speed train whose maximum speed is lower than 200km/h and the high speed train whose maximum speed can reach 500km/h and even higher.

The associate editor coordinating the review of this manuscript and approving it for publication was Montserrat Rivas.

In general, the suspended rotor doesn't contain electrical equipment, so there's no need to consider contactless power supply for it during the operation. Unlike the rotation motion, the maglev train itself contains various electrical equipment serving the levitation and guidance system, braking system and the passengers on vehicle. Hence, it's extremely important to provide power for maglev train. It's common knowledge that traditional wheel rail vehicle applies the pantograph to realize the power supply on board through mechanical contact [7], [8]. Similar to the wheel rail vehicle, the middle-low speed maglev train accomplishes the power supply on board through the mechanical contact between the collector and power rail. For the high speed maglev train, a higher speed operation will bring great challenges for the contact power supply including friction, high temperature, strength, tension and so on. Therefore, there is an urgent need for a contactless power supply system.

There exist two technical routes for the high speed maglev train including EDS SC-Maglev from Japan and EMS Transrapid from German. The SC-Maglev L0 is levitated by the cryogenic superconducting magnets and driven by the synchronous linear motor without iron core, whose maximum

experiment speed can reach 603km/h [9], [10]. Now it's in the trial operating stage and expected to be available commercially in 2027. The EMS Transrapid TR08 is levitated by the electromagnets and driven by the synchronous linear motor with iron core, whose maximum experiment speed can reach 505km/h and maximum operation speed can reach 430km/h [11], [12]. So far it has been operating commercially for near 19 years in Shanghai, China.

In recent years, researchers have done a lot of research work on various systems and field of maglev train. In order to ensure the stable operation at a high speed, a variety of advanced control algorithms of levitation and guidance system have been proposed and investigated [13], [14]. Meanwhile, vehicles dynamics playing an important role in the stability and comfort has been intensive study with the establishment of accurate and comprehensive dynamic model [15]. In addition, the technologies related to propulsion system are also taken seriously, such as the novel positioning sensor, synchronous linear motor and so on [16], [17]. However, there are few researches on contactless power supply system of maglev train at high speed, especially the linear generators. Up to now, there are two types of linear generators to be applied in EDS SC-Maglev and EMS Transrapid to provide power contactless for vehicle at a high speed. In [18]–[20], a linear generator consisting of three-phase coils is proposed for EDS SC-Maglev, which is integrated into the superconducting magnet. Researchers investigate its characteristics and design the corresponding PWM converter. In addition, some advanced control methods are proposed to improve the performance of power supply system on board. In [21], a method combining with the magnetic coupling resonant wireless power transfer technology is proposed based on the mechanical structure of the high speed maglev train in Shanghai, China. Researchers analyze the output power and efficiency of the system and validate them through simulation. Although the analysis results show that it can meet the power supply demand, it has not been applied to vehicle and verified by experiments. In [22], [23], the electromotive force of a linear generator consisting of one-phase coil for EMS Transrapid is calculated by finite element model. The impact factors including air gap, excitation current, speed and others are analyzed carefully. However, the mathematic models of magnetic field and induced voltage are not established. What's more, the experiments to validate the analysis results are not performed.

With the pursuit of speed, a 600km/h EMS maglev train is researched and manufactured in progress, whose diagram of power supply on board is shown in Fig. 1. There are two power supply techniques to applied on maglev train based on the speed including LIG and collector. When the speed is lower than 150km/h, the capacity of power generating for LIG is lower and can't meet the electricity demand on board. So the collector on vehicle and power rail on ground is applied to transfer the power to vehicle through the contact between them, which is only used in the enter and exit station commonly [24]. When the speed is higher than 150km/h, the

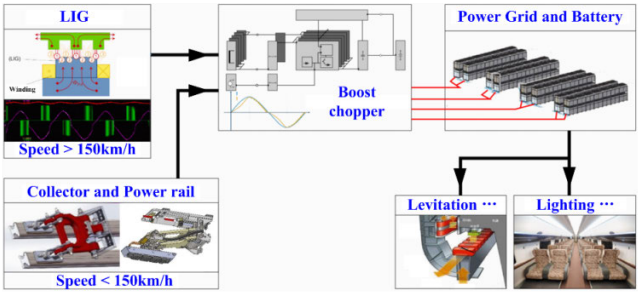

FIGURE 1. Diagram of power supply on board.

LIGs possess the capacity to generate the sufficient power for vehicle, which can cancel the power rail and make it more economical. At a high speed, the power generated by the LIGs is dealt with the boost chopper and transferred to the power grid and battery providing power for the equipment on vehicle such as levitation system, guidance system, braking system, lighting system and so on. Therefore, the characteristics of LIG closely related to the power supply capacity and system parameter matching are the basis of design of the power supply system on board and should be investigated carefully.

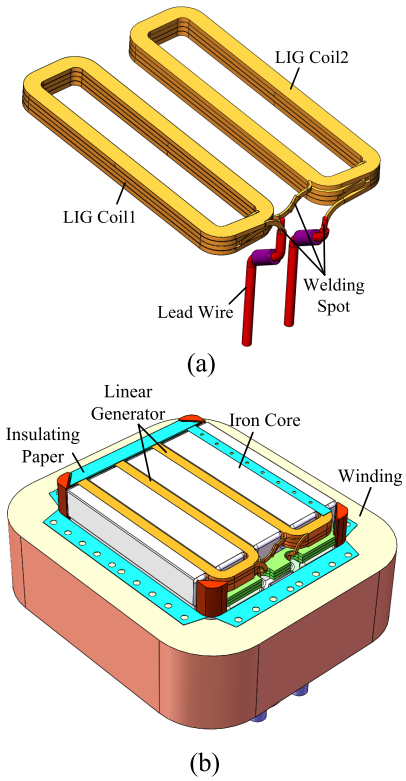

FIGURE 2. Structure diagrammatic sketch of LIG. (a) LIG. (b) Levitation magnet pole.

II. CONFIGURATION AND WORKING PRINCIPLE

A. CONFIGURATION

As Fig. 2 shows, the LIG is composed of two coils wound by enameled wire and two lead wires. Two coils are connected

in series through welding as well as the coil and the lead wire. The LIG is inserted in the iron core of levitation magnet pole to share the magnetic field of levitation magnet pole together. The coils are shaped rectangle to match the groove of iron core better under the effect of a special mould. There exists a layer insulating paper between the LIG coils and the iron core to protect from high-voltage breakdown. The lead wires pass through the iron core and lead out from the bottom making it convenient to output voltage.

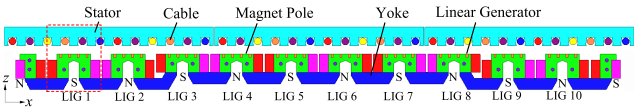

FIGURE 3. Linear motor and levitation magnet.

B. WORKING PRINCIPLE

In the high speed maglev train system, the levitation, propulsion and electric power generation functions are integrated together and accomplished by the linear motor composed of stator pack and levitation magnet shown in Fig. 3. The stator pack includes stator and cables. The levitation magnet includes 10 main magnet poles with LIGs, 2 end magnet poles without LIG and 9 yokes connecting the neighbor magnet poles. When the levitation magnet is powered by direct current, the excitation magnetic field between the magnet pole and the stator will generate. Then the magnetic force in the z direction achieves the levitation function. Subsequently the stator cables are powered by three phase current and the travelling wave magnetic field produced will interact with the excitation magnetic field. Then the magnetic force in the x direction achieves the propulsion function.

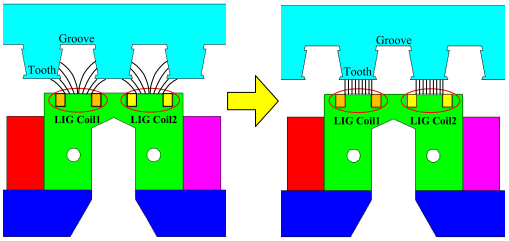

FIGURE 4. Diagram of LIG magnetic flux.

The LIG located in the coupling magnetic field will translate along the x direction with the levitation magnet. When the LIG is in different position, the magnetic flux through its coils are also different. As Fig. 4 shows, when the coil 1 and coil 2 are confronted with the stator grooves, their magnetic fluxes are minimized. When the coil 1 and coil 2 are confronted with the stator teeth, their magnetic fluxes are maximized. Therefore, the magnetic fluxes of LIG varies continuously and periodically with the translation of levitation magnet, which will make the LIG generate an alternating induced voltage. Eventually, the induced voltage is processed by the boost chopper and converted to a 440V DC voltage used for power supply on board.

III. MATHEMATIC MODELING

According to the working principle, it's the magnetic flux alternation that is the fundament of the induced voltage of LIG generating. In this section, the magnetic circuit and voltage models are established to analyze the principle and performance of LIG in detail.

A. MAGNETIC CIRCUIT MODEL

In ideal status, the propulsion system will make the component of magnetic flux maximum value in the x direction and zero in the y direction through the current control for stator cables. The travelling wave magnetic field will pass through LIG coils rarely, and then the performance of LIG is mainly affected by the excitation magnetic field. Consequently, the travelling wave magnetic field can be ignored in the magnetic circuit model. The 12 magnet poles in levitation magnet are divided into the left and right half parts averagely and powered by two controllers respectively. Due to the similarity of two parts, just half a magnetic circuit model is established to simplify the calculation. The magnetic flux paths of the half levitation magnet are shown in Fig. 5. The corresponding equivalent magnetic circuit is also built and shown in Fig. 6.

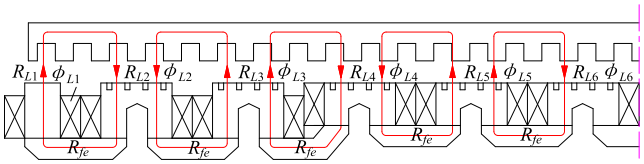

FIGURE 5. Magnetic flux of half levitation magnet.

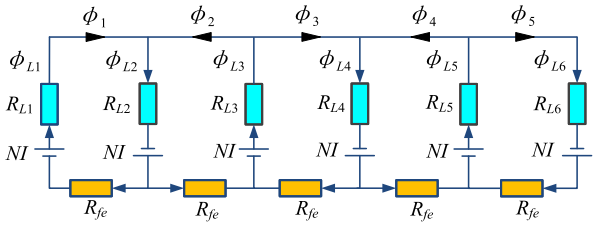

FIGURE 6. Equivalent magnetic circuit of half levitation magnet.

In the magnetic circuit model, NI is the ampere turns of the magnet pole. $R_{Li}\,(i = 1, 2, \cdots, 6)$ is the reluctance of the magnetic gap corresponding to the magnet pole. R_{fe} is the equivalent reluctance of iron cores. $\phi_{Li}\,(i = 1, 2, \cdots, 6)$ is the magnetic flux of the magnetic gap corresponding to the magnet pole. $\phi_i\ (i = 1, 2, \cdots, 5)$ is the magnetic flux of stator in the different magnetic circuits. To simplify the calculation, the leakage fluxes are considered by an equivalent leakage coefficient σ approximately. Based on Kirchhoff's voltage and current law, the equation (1) can be derived.

$$A\phi = B/\sigma \tag{1}$$

where the array

$$A=\begin{bmatrix} R_{L1}+R_{L2}+R_{fe} & R_{L2} & 0 & 0 & 0 \\ R_{L2} & R_{L2}+R_{L3}+R_{fe} & R_{L3} & 0 & 0 \\ 0 & R_{L3} & R_{L3}+R_{L4}+R_{fe} & R_{L4} & 0 \\ 0 & 0 & R_{L4} & R_{L4}+R_{L5}+R_{fe} & R_{L5} \\ 0 & 0 & 0 & R_{L5} & R_{L5}+R_{L6}+R_{fe} \end{bmatrix}.$$

The vector consisting of the magnetic flux ϕ_i $(i = 1, 2, \cdots, 5)$

$$\phi = \begin{bmatrix} \phi_1 & \phi_2 & \phi_3 & \phi_4 & \phi_5 \end{bmatrix}^T.$$

The vector consisting of the ampere turns

$$B = \begin{bmatrix} 2NI & 2NI & 2NI & 2NI & 2NI \end{bmatrix}^T.$$

So the flux ϕ_i $(i = 1, 2, \cdots, 5)$ can be calculated as

$$\phi = A^{-1}B/\sigma \tag{2}$$

The relationship of the magnetic fluxes ϕ_{Li} $(i = 1, 2, \cdots, 6)$ and ϕ_i $(i = 1, 2, \cdots, 5)$ is shown in equation (3) as follows

$$\phi_L = \begin{bmatrix} \phi_{L1} & \phi_{L2} & \phi_{L3} & \phi_{L4} & \phi_{L5} & \phi_{L6} \end{bmatrix}^T = C\phi \tag{3}$$

where the array

$$C = \begin{bmatrix} 1 & 0 & 0 & 0 & 0 \\ 1 & 1 & 0 & 0 & 0 \\ 0 & 1 & 1 & 0 & 0 \\ 0 & 0 & 1 & 1 & 0 \\ 0 & 0 & 0 & 1 & 1 \\ 0 & 0 & 0 & 0 & 1 \end{bmatrix}.$$

Thus the magnetic flux ϕ_{Li} related to the performance of LIG can be obtained. In fact, it's difficult to calculate the reluctance R_{Li} because the magnet pole and stator core is discontinuous under the influence of the cogging structure Thus, the magnetic flux ϕ_{Li} distribution is relatively complex and difficult to solve. In order to analyze the magnetic flux more accurately, the magnetic field between stator and magnet is simulated by 2D finite element model and the result is shown in Fig. 7 (a). Magnetic flux ϕ_{Li} starting from the magnet pole passes through the magnetic gap and divide into two paths ϕ_i and ϕ_{i-1} when get into the stator. While the magnetic gap is a combination of the gaps with different structures including the gap of magnet pole core and stator tooth, the gap of magnet pole core and stator grooves and the gap of LIG grooves and stator tooth. Therefore, the magnetic flux ϕ_{Li} can be refined further and classified into three types named main flux, stray flux and LIG flux respectively shown in Fig. 7 (b).

Based on the three types of equivalent magnetic flux distribution, the reluctance R_{Li} can be taken as three reluctances R_{i1}, R_{i2} and R_{i3} in parallel shown in Fig. 8. So the reluctance R_{Li} in array A can be calculated as

$$R_{Li} = R_{i1}//R_{i2}//R_{i3} \quad (i = 1, 2, \cdots, 6) \tag{4}$$

where R_{i1}, R_{i2} and R_{i3} are the reluctances of the equivalent gaps corresponding to main flux, stray flux and LIG flux respectively.

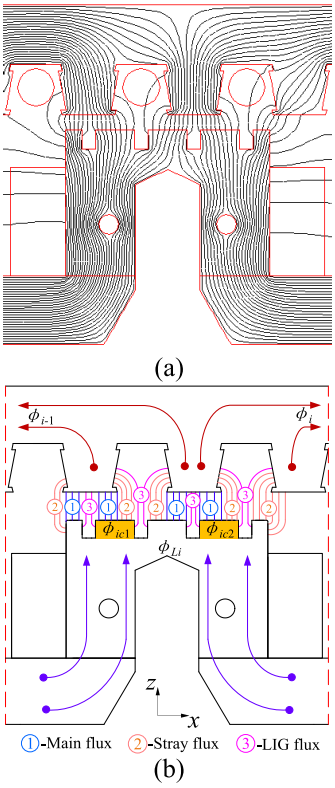

FIGURE 7. Magnetic flux distribution. (a) Simulated magnetic flux. (b) Equivalent magnetic flux.

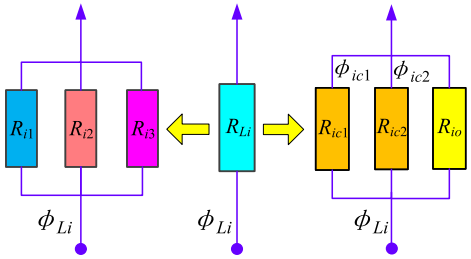

FIGURE 8. Reluctance of magnetic gap.

For the induced voltage, it's the magnetic fluxes through LIG coils ϕ_{ic1} and ϕ_{ic2} need to be analyzed shown in Fig. 7 (b). So the magnetic flux ϕ_{Li} calculated is divided into three parts including magnetic fluxes ϕ_{ic1}, ϕ_{ic2} and others. The corresponding reluctances are R_{ic1}, R_{ic2} and R_{io} shown in Fig. 8. Then the magnetic fluxes through LIG coils can be given by

$$\phi_{ic1} = \frac{\phi_{Li}R_{Li}}{R_{ic1}}, \quad \phi_{ic2} = \frac{\phi_{Li}R_{Li}}{R_{ic2}} \quad (i = 2, 3, \cdots, 6) \tag{5}$$

B. INDUCED VOLTAGE MODEL

For convenience, we just analyzed the magnetic field at a certain time in section III. A. In fact, the induced voltage of LIG generating is a dynamic process. When the levitation magnet translates in the x direction, the reluctances R_{Li}, R_{ic1} and R_{ic2} will change in real time, resulting in the magnetic

fluxes ϕ_{ic1}, ϕ_{ic2} alternation. So the reluctances and magnetic fluxes are the functions of the displacement x. According to the Faraday's Law of electromagnetic induction, the induced voltage can be calculated as

$$U_i = N_L \left[\frac{d\phi_{ic1}(x)}{dt} + \frac{d\phi_{ic2}(x)}{dt} \right] \quad (i = 2, 3, \cdots, 6) \quad (6)$$

where N_L is the turns of LIG coil and $dt = dx/v$. v is the speed of magnet in the x direction. Then the formula (6) can be expressed as

$$U_i = N_L v \left[\frac{d\phi_{ic1}(x)}{dx} + \frac{d\phi_{ic2}(x)}{dx} \right] \quad (i = 2, 3, \cdots, 6) \quad (7)$$

Based on the equation (2), (3) and (5), the formula (7) can be further simplified as

$$U_i = N_L N I v f(x) \quad (i = 2, 3, \cdots, 6) \quad (8)$$

where $f(x)$ represents a function of the displacement x, as well related to the magnetic gap, so the induced voltage varies with the position. As described in the working principle, the LIG coils will pass the grooves and teeth periodically with the movement of levitation magnet. Therefore, the induced voltage should be a period function of x when the magnetic gap is a fixed value or fluctuates in a small range. The period is the width of a groove and a tooth. Normally, the magnetic gap will be maintained near the nominal value during the maglev train operating. So the induced voltage of LIG is linear with not only the turns and speed of itself but also the turns and current of levitation magnet, which means that the power generating capacity of LIG will be affected by the levitation magnet performance.

IV. ANALYTICAL AND NUMERICAL METHOD

As Fig. 7 (b) shows, the magnetic fluxes through LIG coils ϕ_{ic1} and ϕ_{ic2} are composed of a certain amount of main fluxes, stray fluxes and LIG fluxes together, which will change with the position of magnet pole. Actually, it's much difficult to calculate the magnetic fluxes ϕ_{ic1} and ϕ_{ic2} by analytical method accurately, especially when the magnet poles translate. Consequently, the numerical method is selected to assist in the analysis of the magnetic flux distribution between the magnet and stator.

A. MAGNETIC FIELD ANALYSIS

For the linear motor and levitation magnet, the accuracy of 2D finite element model is close to that of 3D finite element model due to the uniformity of its cross section in the y direction. To get the data of magnet field conveniently and consider the efficiency of calculation simultaneously, a 2D finite element model of levitation magnet and stator is established. The main parameters are shown in Fig. 9 and Table 1. The Plane45 elements and nonlinear material whose permeability are defined by BH curves are adopted in the model.

The PATH of command in ANSYS is applied to acquire the magnetic flux density. A single magnet pole is taken as an example to illustrate the magnetic flux distribution, in which two LIG coils correspond two paths. As Fig. 10 shows, the path 1 A_1B_1 and path 2 A_2B_2 are built on the surface of iron core. The analysis results of the magnetic flux density can be mapped to the paths. And then, the magnetic flux density B in the y direction versus the displacement x_l curves can be obtained, which is the main magnetic field for LIG to generate induced voltage.

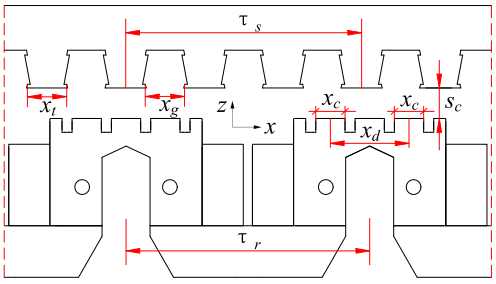

FIGURE 9. Main parameters.

TABLE 1. Parameters of LIG.

Polar distance of stator, τ_s/mm	258
Polar distance of magnet, τ_r/mm	266.5
Tooth width of stator, x_t/mm	43
Groove width of stator, x_g/mm	43
Core width of LIG coil, x_c/mm	32
Distance of LIG coils, x_d/mm	86
Thickness of iron core, l/mm	170
Nominal magnetic gap, s_c/mm	12.5
Nominal current of magnet, I/A	25
Speed of magnet, v/(km/h)	600
Turns of magnet pole, N	300
Turns of LIG coil, N_L	28

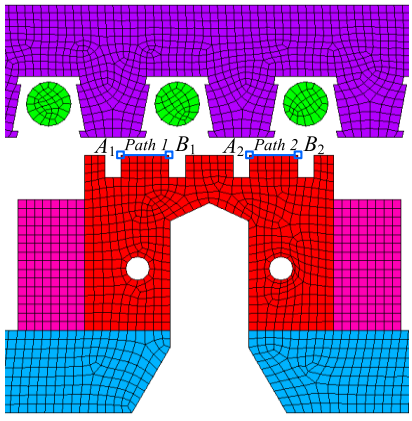

FIGURE 10. Partial 2D finite element model.

Based on the relationship of B-x_l, the magnetic fluxes through LIG coils in a certain position can be expressed as

$$\phi_{icj} = \int_0^{x_c} B_{icj}(x_l) l dx_l \quad (j = 1, 2) \quad (9)$$

Although the analytic expression of function $B_{icj}(x_l)$ can't be given accurately, it can be discretized and linearized.

When the magnetic flux density is mapped to the paths, the number of mapping points on the path can be decided as needed. The function $B_{icj}(x_l)$ is also discretized into the corresponding number of sections. Then the magnetic fluxes can be calculated by linearization in every discrete section. So the formula (9) can be replaced by

$$\phi_{icj} = \frac{x_c l}{2(M-1)} \sum_{k=1}^{M-1} [B_{icj}(x_k) + B_{icj}(x_{k+1})] \quad (j = 1, 2) \tag{10}$$

where M is the number of mapping points and x_k is one of the points. When the value of M is larger, the calculation results of magnetic flux is more accurate. In the following, a demonstration of $B_{icj}(x_l)$ in the position shown in Fig. 10 is given. The value of M is 33 and the curves are shown in Fig. 11.

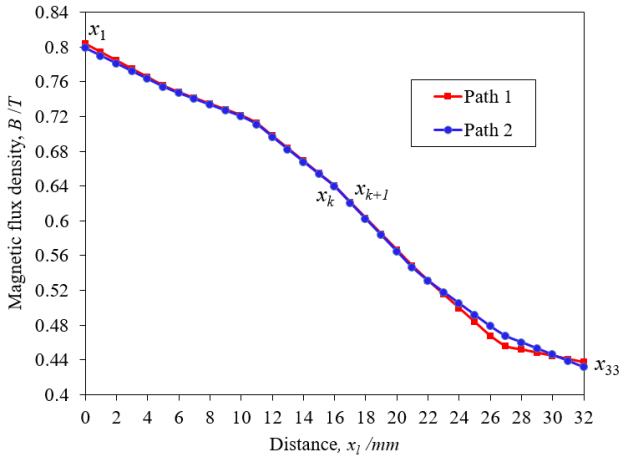

FIGURE 11. ***B*-x_l characteristics of paths.**

In this case, the magnetic fluxes of LIG can be calculated based on the formula (10).

$$\phi_{ic1} = \frac{x_c l}{64} \sum_{k=1}^{32} [B_{ic1}(x_k) + B_{ic1}(x_{k+1})]$$

$$\phi_{ic2} = \frac{x_c l}{64} \sum_{k=1}^{32} [B_{ic2}(x_k) + B_{ic2}(x_{k+1})]$$

B. INDUCED VOLTAGE ANALYSIS

Similar to the magnetic fluxes calculation, the induced voltage is also calculated in a discrete way. For example, the magnetic flux of LIG coil is $\phi_{icj}(t)$ at a certain point. Based on formula (6), the discretization formula of the induced voltage can be derived

$$U_i(t) = \sum_{j=1}^{2} \frac{\phi_{icj}(t + \Delta t) - \phi_{icj}(t)}{\Delta t} \tag{11}$$

where Δt represents a very small time increment, which can be decided according to the actual speed. In this part, the induced voltage of one LIG with the speed of 600km/h is calculated in a period by the analytical and numerical method. The value of Δt is selected as 0.01ms. Meanwhile, the induced voltage is simulated by the Ansoft model and both results are shown in Fig. 12.

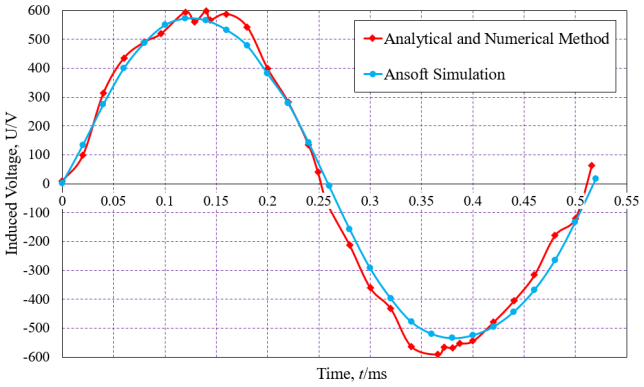

FIGURE 12. **Induced voltage characteristics.**

The polar distance of stator is 258mm and the propulsion period is 516mm, so the propulsion frequency is 323Hz at the speed of 600km/h. As previously described, the period of induced voltage is the width of a groove and a tooth, of which the value is 86mm. Therefore, the theoretical value of its frequency should be 1.938kHz and 6 times of the propulsion one. As Fig. 12 shows, the induced voltage results of LIG analyzed by two methods at the speed of 600km/h have a good consistency, including the amplitude and frequency. The frequency is about 1.92kHz nearly identical with the theoretical value. The amplitude is about 598V, which is proportional to the speed based on the formula (8).

To summarize, the induced voltage characteristic can be expressed simply as $U_{im} = 3.6v$ and $f_{LIG} = 6f_{pro}$. Where U_{im} represents the induced voltage amplitude. f_{LIG} represents the induced voltage frequency. f_{pro} represents the propulsion frequency and $f_{pro} = 0.5v/\tau_s$. For example, when the speed is 150km/h, the induced voltage amplitude is 150V and the frequency is 484Hz.

C. OUTPUT CURRENT ANALYSIS

Although the characteristics analysis of the induced voltage is performed in the open circuit state, the output characteristics in the closed circuit is also important, and then we analyze the output current of one LIG at different loads in this section. As mentioned earlier, the power for levitation system is from LIG, so the different loads within the load range of levitation magnet are selected to analyze the corresponding output current and the results at the speed of 600km/h are shown in Fig. 13. When the inductive load is very low or even zero, the output current and induced voltage have the same phase and a linear relationship. However, due to the coil structure and magnetic flux loop, the levitation magnet will have a large inductive load, and the inductance of half a levitation magnet can reach about 1.5H. At this moment, a phase delay between the output current and induced voltage will appear

and the current amplitude will decrease with the increase of inductance. Therefore, the generating capacity and load condition of LIG need to be considered at the same time in the design of power supply system on board.

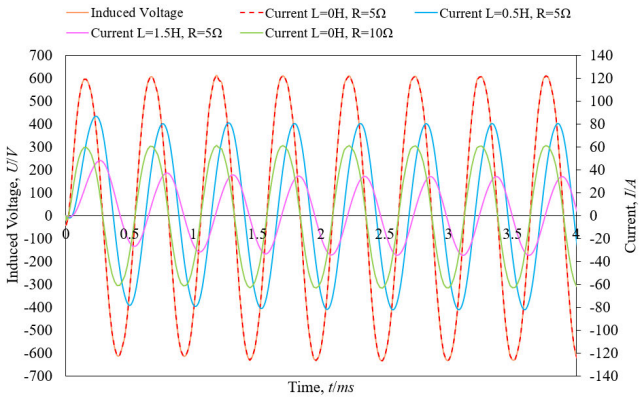

FIGURE 13. Output current at different loads.

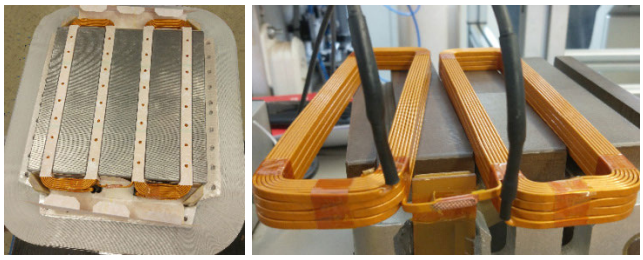

FIGURE 14. Prototype of LIG.

V. PROTOTYPE AND EXPERIMENT

To validate the results of the analytical and numerical method, some relevant experiments are carried out including magnetic field and induced voltage tests. The prototype of LIG is shown in Fig. 14. Since the LIG is installed in levitation magnet pole and its work depends on the magnetic field generated by levitation magnet, a whole magnet rather than just LIG is taken as the experiment object.

A. MAGNETIC FIELD TEST

As aforementioned, it's significant to analyze the magnetic fluxes distribution between levitation magnet and stator accurately for the induced voltage calculation of LIG. In this section, the magnetic flux density is measured to validate the results from 2D finite element model. Similar to the LIG paths, another path along the whole levitation magnet model is established at the magnetic gap to assist to acquire the magnetic flux density data. The performance test bench of magnet shown in Fig. 15 is applied on the measurement of magnetic flux density [25]. Firstly, make sure the nominal magnetic gap 12.5mm through adjusting the stator of bench. Then, a DC current consistent with the parameter of 2D finite element model is supplied to the levitation magnet. Finally, the magnetic field sensor translates between the levitation magnet and stator measuring the magnetic flux density. The contrast between the simulation and experiment results are revealed in Fig. 16.

FIGURE 15. Performance test bench of magnet.

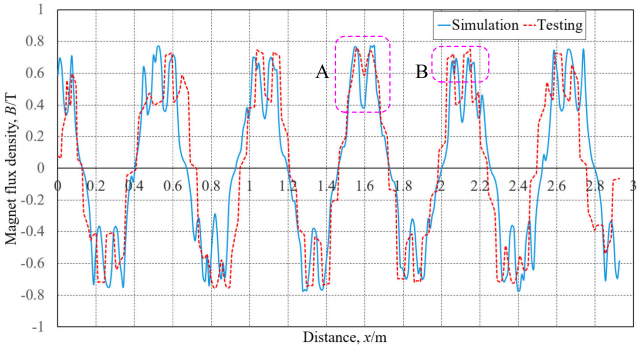

FIGURE 16. Magnetic flux density in the *y* direction.

The characteristic of *B*-*x* analyzed by 2D finite element has a good agreement with the experiment one. At the beginning and end of the levitation magnet, there are slight displacement deviation between two results. The main reason is that the magnetic field sensor is driven by the motor and conveyor belt. So it's impossible to guarantee a uniform motion due to the acceleration, deceleration and vibration. As Fig. 3 shows, the magnetic polarities of the magnet poles are N/S alternating, hence the magnetic flux density results exist the positive and negative wave peaks whose absolute value is in the range of 0.6T $\sim$ 0.8T. In addition, there are two types of fluctuations in the peaks, such as position A and position B shown in Fig. 16. The fluctuation of position A is caused by the cogging structure of the stator and the one of position B is caused by the installation slots of the LIG coils.

B. INDUCED VOLTAGE TEST

To validate the induced voltage characteristics of LIG, the actual induced voltages of two neighbor LIGs are monitored in real time during the commissioning of the 600km/h EMS maglev prototype. Limited by the length of the commissioning track, the maximum test speed of train can just reach 50km/h. The induced voltages of LIGs at the speeds of 25km/h and 50km/h are collected with a sampling frequency of 50kHz and dealt with a low pass filtering. The voltage waveforms are shown in Fig. 17. Furthermore, the result of analytical and numerical method is processed based on the relationship of induced voltage and speed analyzed in part IV. B and the comparison with the test one in one period is shown in Fig. 18.

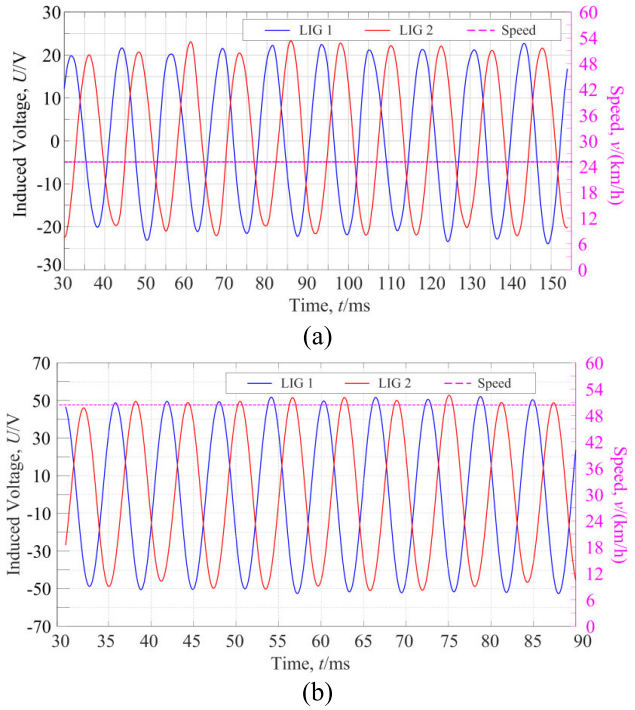

FIGURE 17. Testing results in real vehicle. (a) Induced voltage at 25km/h. (b) Induced voltage at 50km/h.

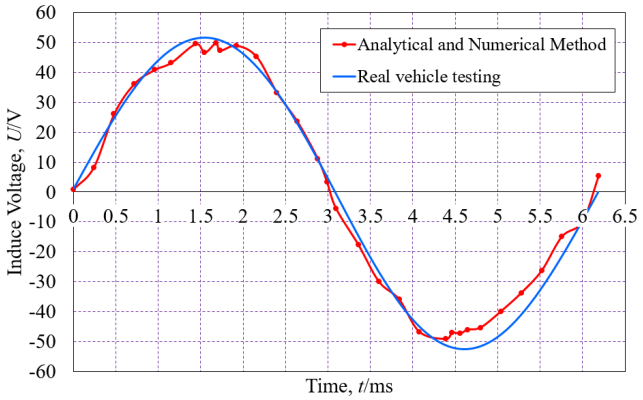

FIGURE 18. Induced voltage characteristics.

The voltage frequencies of LIG 1 and LIG 2 obtained through Fourier transform of the test data are approximate 80Hz for the speed 25km/h and 160Hz for the speed 50km/h respectively, which are all close to the theoretical values. The voltage amplitude at the speed of 50km/h is near the theoretical value 50V. The voltage amplitude at the speed of 25km/h is slightly lower than the theoretical value 25V. The main reason is that the dynamic load of vehicle is relatively small at a lower speed resulting in a smaller current of levitation magnet than the nominal value. As the formula (8) revealed, the induced voltage will decrease with the decrease of the levitation magnet current. The induced voltage waveform in one period analyzed by the analytical and numerical method has a good agreement with the test one at the speed of 50km/h, so the method used to analyze the characteristics of LIG is validated.

VI. CONCLUSION

In this paper, the LIG applied in high speed maglev train is introduced, whose characteristics are analyzed by equivalent magnetic circuit method, analytical and numerical method and real vehicle testing.

(1) The mathematic and finite element model are established to analyze the characteristics of LIG. The magnetic field and induced voltage calculated by analytical and numerical method are verified by the experiments on the performance test bench of magnet and real vehicle indicating that the analysis results are reasonable.

(2) The method combining the analytical and finite element methods possesses the advantages of them. The relationships between the induced voltage and parameters are presented intuitively in the analytical formulas and the magnetic field is analyzed accurately by the finite element model. It makes the design, analysis and optimization of LIG more efficient.

(3) The amplitude and frequency of the induced voltage are proportional to the speed when the structure and performance parameters of levitation magnet are determined.

(4) The characteristics of induced voltage are not only related to its own parameters but also to the performance of the levitation magnet generating the main magnetic field for LIG. Therefore, the impact factors are needed to take into consideration simultaneously during the design and optimization of LIG, such as the turns of itself, the ampere turns and structure parameters of levitation magnet, the magnetic gap and the maximum operation speed of maglev train.

REFERENCES

[1] B. Han, S. Zheng, Y. Le, and S. Xu, "Modeling and analysis of coupling performance between passive magnetic bearing and hybrid magnetic radial bearing for magnetically suspended flywheel," *IEEE Trans. Magn.*, vol. 49, no. 10, pp. 5356–5370, Oct. 2013.

[2] C. Peng, J. C. Fang, and S. Xu, "Composite anti-disturbance controller for magnetically suspended control moment gyro subject to mismatched disturbances," *Nonlinear Dyn.*, vol. 79, no. 2, pp. 1563–1573, Jan. 2015.

[3] L. Zhai, J. Sun, X. Ma, W. Han, and X. Luo, "Thermal–structure coupling analysis and multi-objective optimization of motor rotor in MSPMSM," *Chin. J. Aeronaut.*, vol. 32, no. 7, pp. 1733–1747, Jul. 2019.

[4] H.-W. Lee, K.-C. Kim, and J. Lee, "Review of maglev train technologies," *IEEE Trans. Magn.*, vol. 42, no. 7, pp. 1917–1925, Jul. 2006.

[5] Y. Luguang, "Progress of the maglev transportation in China," *IEEE Trans. Appl. Supercond.*, vol. 16, no. 2, pp. 1138–1141, Jun. 2006.

[6] L. Yan, "Development and application of the maglev transportation system," *IEEE Trans. Appl. Supercond.*, vol. 18, no. 2, pp. 92–99, Jun. 2008.

[7] C. Xiao, M. Yang, C. Tan, and Z. Lu, "Effects of platform sinking height on the unsteady aerodynamic performance of high-speed train pantograph," *J. Wind Eng. Ind. Aerodynamics*, vol. 204, Sep. 2020, Art. no. 104284, doi: 10.1016/j.jweia.2020.104284.

[8] M. Carnevale, A. Facchinetti, and D. Rocchi, "Procedure to assess the role of railway pantograph components in generating the aerodynamic uplift," *J. Wind Eng. Ind. Aerodyn.*, vol. 160, pp. 16–29, Jan. 2017.

[9] H. Cho, D. K. Bae, and B. C. Shin, "HTSC levitation experiment with AC current modeling after EDS maglev," *IEEE Trans. Appl. Supercond.*, vol. 17, no. 2, pp. 2095–2098, Jun. 2007.

[10] T. Murai, Y. Sakamoto, S. Fujiwara, and H. Yoshioka, "Harmonic characteristics of SC coil configuration for EDS maglev to reduce leakage flux," *Electron. Commun. Jpn.*, vol. 91, no. 10, pp. 20–27, Oct. 2008.

[11] M. Zhai, Z. Long, and X. Li, "Fault-tolerant control of magnetic levitation system based on state observer in high speed maglev train," *IEEE Access*, vol. 7, pp. 31624–31633, 2019.

[12] M. Zhai, A. Hao, X. Li, and Z. Long, "Research on the active guidance control system in high speed maglev train," *IEEE Access*, vol. 7, pp. 741–752, 2019.
[13] Y. Yang, Z. Long, and Y. Xie, "An improved sliding mode control via discrete time optimal control and its application to magnetic suspension system," *IEEE Access*, vol. 8, pp. 185584–185594, 2020.
[14] C. Chen, J. Xu, G. Lin, Y. Sun, and F. Ni, "Model identification and nonlinear adaptive control of suspension system of high-speed maglev train," *Vehicle Syst. Dyn.*, vol. 7, pp. 1–22, Nov. 2020, doi: 10.1080/00423114.2020.1838564.
[15] Y. J. Li, D. F. Zhou, P. Cui, P. C. Yu, Q. Chen, L. C. Wang, and J. Li, "Dynamic performance optimization of electromagnetic levitation system considering sensor position," *IEEE Access*, vol. 8, pp. 29446–29455, 2020.
[16] X. B. Hong, J. Wu, Y. Z. Zhang, and Y. X. He, "Research on absolute positioning sensor based on eddy current reflection for high-speed maglev train," *Sensor*, vol. 20, no. 18, pp. 1–15, Sep. 2020.
[17] J.-M. Jo, S. Y. Lee, K. Lee, Y. J. Oh, S. Y. Choi, C.-Y. Lee, and K. Lee, "A position estimator using Kalman filter with a data rejection filter for a long-stator linear synchronous motor of maglev," *IEEE Access*, vol. 8, pp. 52443–52451, 2020.
[18] H. Hasegawa and H. Matsue, "Development of a linear generator integrated into an existing superconducting magnet of a yamanashi maglev vehicle," *Quart. Rep. RTRI*, vol. 45, no. 1, pp. 21–25, 2004.
[19] T. Yamamoto, T. Murai, H. Hasegawa, H. Yoshioka, S. Fujiwara, and S. Hatsukade, "Development of distributed-type linear generator with damping Control.," *Quart. Rep. RTRI*, vol. 41, no. 2, pp. 83–88, 2000.
[20] T. Murai, Y. Sakamoto, and H. Hasegawa, "High power factor converter control by instantaneous single-phase current for a maglev system linear generator," in *Proc. Power Convers. Conf.*, New York, NY, USA, Apr. 2007, pp. 1158–1163.
[21] W. Ying, L. Weiguo, H. Hongyun, L. Zongjian, X. Yang, and L. Da, "Research on contactless power supply of high speed maglev train based on MCR-WPT," in *Proc. 14th IEEE Conf. Ind. Electron. Appl. (ICIEA)*, Xian, China, Jun. 2019, pp. 2297–2302.
[22] L. Li and Q. Lu, "Investigation of linear generator for high speed maglev train by 2D finite element model," in *Proc. 12th Int. Symp. Linear Drives Ind. Appl. (LDIA)*, Neuchatel, Switzerland, Jul. 2019, pp. 1–6.
[23] G. Liang, L. Qinfen, and Y. Yunyue, "FEM analysis of the linear generator EMF in maglev," in *Proc. Int. Conf. Electr. Mach. Syst.*, Nanjing, China, 2005, pp. 2112–2115.
[24] X. C. Ma, G. Q. He, D. H. He, C. S. Chen, and Z. F. Hu, "Sliding wear behavior of copper–graphite composite material for use in maglev transportation system," *Wear*, vol. 265, nos. 7–8, pp. 1087–1092, Sep. 2008.
[25] S. S. Ding, J. J. Sun, W. T. Han, G. M. Deng, F. J. Jiang, and C. E. Wang, "Modeling and analysis of a novel guidance magnet for high-speed maglev train," *IEEE Access*, vol. 7, pp. 133324–133334, 2019.

SANSAN DING was born in Hubei, China, in 1967. He received the M.S. degree from Central South University, Hunan, China, in 2000, and the Ph.D. degree from Beijing Jiaotong University, Beijing, China, in 2016.

He is currently the Chief Engineer of the National Engineering Research Center, CRRC Qingdao Sifang Company Ltd., China. His research interest includes the design of high speed maglev system.

WEITAO HAN was born in Shandong, China, in 1989. He received the B.S. degree from Shandong University, Shandong, China, in 2013, and the M.S. degree from Beihang University, Beijing, China, in 2016.

He is currently a Research Member with the Research Department of Maglev Technology, CRRC Qingdao Sifang Company Ltd., China. His research interests include the design of electromagnets and linear motors.

JINJI SUN received the Ph.D. degree in instrument science and technology from Beihang University, Beijing, China, in 2010, where he is currently pursuing the Ph.D. degree.

He is currently a Research Member with the Key National Defense Laboratory of Novel Inertial Instrument and Navigation System Technology, School of Instrumentation Science and Opto-Electronics Engineering, Beihang University, China. His research interests include the design of novel various types of magnetic bearings and brushless DC motors.

FUJIE JIANG was born in Shandong, China, in 1977. He received the B.S. degree from the University of Petroleum, Heilongjiang, China, in 2001.

He is currently the Director of the Research Department of Maglev Technology, CRRC Qingdao Sifang Company, Ltd., China. His research interests include levitation and guidance system control.

GUIMEI DENG was born in Hunan, China, in 1974. He received the B.S. degree from Southwest Jiaotong University, Sichuan, China, in 1998.

He is currently a Research Member with the Research Department of Maglev Technology, CRRC Qingdao Sifang Company Ltd., China. His research interest includes power supply system control.

YUNQI SHI was born in Heilongjiang, China, in 1992. She received the B.S. degree from the China University of Petroleum, Shandong, China, in 2013, and the M.S. degree from the University of Ottawa, Ottawa, Canada, in 2016.

She is currently a Research Member with the National Engineering Research Center, CRRC Qingdao Sifang Company Ltd., China. Her research interest includes high speed rail train technology.